



CENTER FOR CONNECTED AND  
AUTOMATED TRANSPORTATION

Final Report #ICT-21-037  
November 2021



## **Generalized Link-Cost Function and Network Design for Dedicated Truck-Platoon Lanes to Improve Energy, Pavement Sustainability, and Traffic Efficiency**

Yanfeng Ouyang  
George Krambles Endowed Professor  
Rufeng She  
Graduate Research Assistant

## **DISCLAIMER**

Funding for this research was provided by the Center for Connected and Automated Transportation under Grant No. 69A3551747105 of the U.S. Department of Transportation, Office of the Assistant Secretary for Research and Technology (OST-R), University Transportation Centers Program. The contents of this report reflect the views of the authors, who are responsible for the facts and the accuracy of the information presented herein. This document is disseminated under the sponsorship of the Department of Transportation, University Transportation Centers Program, in the interest of information exchange. The U.S. Government assumes no liability for the contents or use thereof.

## **Suggested APA Format Citation:**

She, R., & Ouyang, Y. (2021). *Generalized link-cost function and network design for dedicated truck-platoon lanes to improve energy, pavement sustainability, and traffic efficiency* (Report No. ICT-21-037). Illinois Center for Transportation. <https://doi.org/10.36501/0197-9191/21-037>

## **Contacts**

For more information:

Ruifeng She  
University of Illinois at Urbana–Champaign  
B235 Newmark Civil Engineering Laboratory  
205 North Mathews Avenue, Urbana, IL 61801  
[rshe2@illinois.edu](mailto:rshe2@illinois.edu)  
(217) 300-1488  
<https://ict.illinois.edu>

CCAT  
University of Michigan Transportation Research Institute  
2901 Baxter Road  
Ann Arbor, MI 48152  
[uumtri-ccat@umich.edu](mailto:uumtri-ccat@umich.edu)  
(734) 763-2498  
[www.ccat.umtri.umich.edu](http://www.ccat.umtri.umich.edu)

**TECHNICAL REPORT DOCUMENTATION PAGE**

<b>1. Report No.</b> ICT-21-037	<b>2. Government Accession No.</b> N/A	<b>3. Recipient's Catalog No.</b> N/A	
<b>4. Title and Subtitle</b> Generalized Link-Cost Function and Network Design for Dedicated Truck-Platoon Lanes to Improve Energy, Pavement Sustainability, and Traffic Efficiency		<b>5. Report Date</b> November 2021	
		<b>6. Performing Organization Code</b> N/A	
<b>7. Authors</b> Ruifeng She, Yanfeng Ouyang		<b>8. Performing Organization Report No.</b> ICT-21-037 UILU-ENG-2021-2037	
<b>9. Performing Organization Name and Address</b> Illinois Center for Transportation Department of Civil and Environmental Engineering University of Illinois at Urbana–Champaign 205 North Mathews Avenue, MC-250 Urbana, IL 61801		<b>10. Work Unit No.</b> N/A	
		<b>11. Contract or Grant No.</b> Grant No. 69A3551747105	
<b>12. Sponsoring Agency Name and Address</b> Center for Connected and Automated Transportation University of Michigan Transportation Research Institute 2901 Baxter Road Ann Arbor, MI 48152		<b>13. Type of Report and Period Covered</b> Final Report	
		<b>14. Sponsoring Agency Code</b> Center for Connected and Automated Transportation	
<b>15. Supplementary Notes</b> Funding under Grant No. 69A3551747105 U.S. Department of Transportation, Office of the Assistant Secretary for Research and Technology (OST-R), University Transportation Centers Program. <a href="https://doi.org/10.36501/0197-9191/21-037">https://doi.org/10.36501/0197-9191/21-037</a>			
<b>16. Abstract</b> Recent development of autonomous and connected trucks (ACT) has provided the freight industry with the option of using truck platooning to improve fuel efficiency, traffic throughput, and safety. However, closely spaced and longitudinally aligned trucks impose frequent and concentrated loading on pavements, which often accelerates pavement deterioration and increases the life cycle costs for the highway agency. Also, effectiveness of truck platooning can be maximized only in dedicated lanes; and its benefits and costs need to be properly balanced between stakeholders. This paper proposes a network-design model to optimize (i) placement of dedicated truck-platoon lanes and toll price in a highway network, (ii) pooling and routing of ACT traffic from multiple origins and destinations to utilize these lanes, and (iii) configuration of truck platoons within these lanes (e.g., lateral displacements and vehicle separations). The problem is formulated as an integrated bi-level optimization model. The upper level makes decisions on converting existing highway lanes into dedicated platoon lanes, as well as setting user fees. The lower-level decisions are made by independent shippers regarding the choice of routes and use of platoon lanes vs. regular lanes; and they collectively determine truck traffic in all lanes. Link-cost functions for platoon lanes are obtained by simultaneously optimizing, through dynamic programming, pavement-rehabilitation activities and platoon configuration in the pavement's life cycle. A numerical case study is used to demonstrate the applicability and performance of the proposed model framework over the Illinois freeway system. It is shown that the freight traffic is effectively channelized on a few corridors of platoon lanes and, by setting proper user fees to cover pavement-rehabilitation costs, systemwide improvements for both freight shippers and highway agencies can be achieved.			
<b>17. Key Words</b> Autonomous and Connected Trucks, Truck Platooning, Truck Aerodynamics, Pavement Damage, Optimization		<b>18. Distribution Statement</b> No restrictions. This document is available through the National Technical Information Service, Springfield, VA 22161.	
<b>19. Security Classif. (of this report)</b> Unclassified	<b>20. Security Classif. (of this page)</b> Unclassified	<b>21. No. of Pages</b> 33	<b>22. Price</b> N/A

## **ACKNOWLEDGMENT, DISCLAIMER, MANUFACTURERS' NAMES**

This project was conducted in cooperation with the Center for Connected and Automated Transportation and the Illinois Center for Transportation. The contents of this report reflect the view of the authors, who are responsible for the facts and the accuracy of the data presented herein. The contents do not necessarily reflect the official views or policies of CCAT or ICT. This report does not constitute a standard, specification, or regulation. Trademark or manufacturers' names appear in this report only because they are considered essential to the object of this document and do not constitute an endorsement of the product by CCAT or ICT

# TABLE OF CONTENTS

<b>Chapter 1: Introduction .....</b>	<b>1</b>
<b>Chapter 2: Link-Cost Components for Dedicated Platoon Lanes.....</b>	<b>3</b>
Truck Aerodynamics.....	3
Pavement Damage and Cost .....	4
Preliminary Optimization of Platoon Configuration.....	5
<b>Chapter 3: Generalized Link-Cost Function .....</b>	<b>7</b>
Platoon Configuration and Life Cycle Cost.....	7
Dynamic Program Solution.....	10
<b>Chapter 4: Network Design .....</b>	<b>11</b>
Bi-level Model .....	11
Solution Method .....	14
<b>Chapter 5: Numerical Result .....</b>	<b>15</b>
Optimal Platoon and Link-Cost Function .....	15
Network-level Optimization .....	20
<b>References.....</b>	<b>30</b>

# LIST OF FIGURES

Figure 1. Equation. Air drag cost function.....	4
Figure 2. Equation. IRI definition.....	4
Figure 3. Equation. Maximum IRI over pavement cross-section. ....	4
Figure 4. Equation. Rehabilitation cost definition.....	5
Figure 5. Equation. Vehicle-related cost definition.....	5
Figure 6. Equation. Link flow capacity.....	7
Figure 7. Diagram. Platoon-configuration definition in a dedicated lane.....	8
Figure 8. Equation. Air drag function. ....	8
Figure 9. Equation. Vehicle-related cost function.....	8
Figure 10. Equation. Rehabilitation cost function.....	8
Figure 11. Equation. LCC-minimization program over platoon configurations. Objective function.....	9
Figure 12. Equation. IRI initial condition. ....	9
Figure 13. Equation. Maximum IRI constraint.....	9
Figure 14. Equation. IRI increment conditional on rehabilitation decision. ....	9
Figure 15. Equation. Variable feasible domain definitions. ....	9
Figure 16. Equation. Bellman equation.....	10
Figure 17. Equation. Travel time cost function. ....	12
Figure 18. Equation. Total link flow definition. ....	12
Figure 19. Equation. Upper-level objective function. ....	12
Figure 20. Equation. Upper-level variable domain definition.....	13
Figure 21. Equation. Lower-level objective function. ....	13
Figure 22. Equation. Flow conservation constraint. ....	13
Figure 23. Equation. Link flow capacity constraint. ....	13
Figure 24. Equation. Infeasible link flow constraint.....	13
Figure 25. Equation. Lower-level variable domain definition.....	13
Figure 26. Graph. Optimal platoon configuration and rehabilitation schedule over the planning horizon for AADT = 40,000 and 100,000.....	17
Figure 27. Graph. Link-cost components for platooned truck traffic. ....	19
Figure 28. Graph. Link-cost function. ....	20
Figure 29. Diagram. The Illinois network. ....	22
Figure 30. Diagram. Network design and flow pattern. ....	24
Figure 31. Graph. Life cycle cost components breakdown for five cases. ....	25
Figure 32. Graph. Network design and flow pattern. ....	27
Figure 33. Graph. Percentages of cost reduction and lane-mile conversion under light demand. ....	28
Figure 34. Graph. Percentages of cost reduction and lane-mile conversion under a range of demand levels....	29

## **LIST OF TABLES**

Table 1. Representative Platoon Configurations and Pavement-Rehabilitation Thresholds.....	18
Table 2. Origin–destination demand matrix in AADT (scaled from 2012 WIM data) .....	23

# CHAPTER 1: INTRODUCTION

Although modern logistics systems are often based on intermodal networks consisting of highway, railroad, air, and maritime components, for continental nations, freight traffic largely relies on heavy-duty trucks for short- to medium-range shipments. The share of highway transportation in total inland freight-shipment ton-mileage in 2018 is 76.5% for Europe [1] and 60% for the United States [2]. Automation technology in the automobile industry, therefore, holds a strong promise to revolutionize safety and efficiency of freight traffic, e.g., by reducing and even eliminating human factors in driving. As such, vehicle motion becomes predictable and controllable to an extent that operations previously considered dangerous with human drivers, such as platooning at a high speed with a very small clearance, can now be practiced safely. A research team led by Tsugawa et al. [3], for example, conducted experiments in 2011 with automated trucks running at 80 km/h with a clearance of merely 4.7 m.

One of the most quantifiable economic benefits of truck platooning is fuel savings. Aerodynamic efficiency has not been a crucial consideration in the design of heavy-duty trucks, as the emphasis is normally given to load-carrying capacity and mechanical efficiency. Consequently, a large portion of fuel consumption can be attributed to air pressure drag [4], which thus leaves a significant potential for fuel savings through truck platooning. Zabat et al. [5] experimented with a platoon of four trucks and showed that aligning vehicles with a small clearance favored fuel savings. In 2012, the California PATH Program experimented with a three-truck platoon with a clearance of 6 m and saw a 10% reduction in fuel consumption [6]. Various additional experiments have been carried out in the following years. Bhoopalam et al. [7] gave a comprehensive review of these truck-platooning efforts, with particular focus on fuel-economy improvements. The air drag reduction was found to be largely dependent on the relative position of the trucks in a platoon, which is consistent with the findings for intermodal trains (e.g., Lai et al. [8]). Based on this result, Gungor et al. [9] used computational fluid dynamics simulations to evaluate air drag reduction on a pair of trucks at various platoon positions and developed a prediction model for general truck platoons.

The benefit in fuel savings does not come free. Channelizing trucks closely in a strict alignment causes frequent and concentrated loading pattern on the pavements. This fact, combined with the heavy weight of freight trucks, has a significant impact on the durability and service life of the pavement structure. Noorvand et al. [10] quantified this effect and compared it with human-driven trucks (whose lateral position in a lane is random). In particular, the small clearance between platooned trucks reduces the resting period for pavements to recover from traffic loading, which hinders the self-healing effect of asphalt pavements [11]. Based on the *Mechanistic-Empirical Pavement Design Guide (MEPDG)*, Gungor and Al-Qadi [12] developed a prediction model, known as Wander 2D, to capture this effect and predict service life under a given platooning configuration. In [9], further efforts were made to determine the optimal platoon configuration (e.g., lateral displacements and vehicle separations) that balances the trade-off between fuel savings and pavement damage.

Although operational-level understanding of truck platooning has received considerable attention, there has been relatively less literature on exploration at the strategic level; e.g., deployment of dedicated platoon lanes in a highway network—it is intuitive that efficiency of truck platooning can

be maximized only in dedicated lanes where interference from conventional vehicles is avoided ([6], [13]). Hajibabai et al. [14] developed integrated design models to optimize freight supply-chain networks and truck-routing decisions, which explicitly consider optimization of pavement-rehabilitation activities in a life cycle. Larsson et al. [15] investigated a vehicle-routing problem with platooning options for a finite list of truck-trip missions. Along this line, Luo et al. [16] considered the routing problem with speed options. Sokolov et al. [17] explored simultaneously platoon coordination and vehicle routing. A recent study by Noruzoliae et al. [18] investigated the network traffic-equilibrium problem with the option of platooning on links. However, the link-cost function considers only travel time and a fixed value of fuel savings from platooning but no pavement-related terms. From a microscopic perspective, each truck enjoys fuel savings differently, depending on its position within a platoon. Sun and Yin conducted a series of studies investigating the decision game among platooned trucks and proposed utility-redistribution mechanics to achieve equilibrium [19], [20].

To the best knowledge of the authors, no existing literature has studied network design for dedicated platoon lanes under traffic equilibrium with explicit consideration of (i) the benefit and cost trade-offs of platooning operations (i.e., fuel savings vs. accelerated pavement deterioration), as well as redistribution of benefits through lane-user fees; and (ii) simultaneous optimization of platoon configuration and pavement-rehabilitation schedules that characterize the link-cost functions for a range of traffic volumes in a life cycle. This work thus aims to fill these gaps in the following respects. First, a generalized link-cost function is characterized for truck-platoon lanes that considers the trade-off between fuel savings, travel delay, and pavement-rehabilitation costs under a range of truck flow. In doing so, our method uses a combination of (a) an MEPDG model for pavement, (b) a computational fluid dynamics model for energy consumption, and (c) a dynamic programming-based framework to minimize the life cycle cost (including energy and pavement) by optimizing platoon configuration and pavement-rehabilitation schedule simultaneously. The resulting link-cost functions are then fed into a bi-level network-design and traffic-assignment model to determine the optimal layout of platoon lanes in a general highway network, and the corresponding equilibrium traffic. Effective solution algorithms based on meta-heuristic methods are proposed to solve the bi-level model. Finally, the proposed model framework was implemented on the Illinois freeway network to show its applicability and also to draw a number of insights as to the best operational strategy (e.g., toll price) and potential gain from platooned truck traffic expecting growing logistic demand.

## CHAPTER 2: LINK-COST COMPONENTS FOR DEDICATED PLATOON LANES

The impact of truck platooning on transportation operations is multifaceted. As discussed, fuel consumption due to aerodynamic drags is expected to be minimized when trucks are aligned perfectly, with a minimum clearance inside a compact platoon. An additional operational benefit is the increase in truck flow at any given speed because platooned trucks can travel in a higher density—or in other words, platooned traffic can travel at a higher speed for any given density. However, the immediate drawback of such operations lies in the accelerated damage accumulation in the pavement, which consequently induces additional pavement-rehabilitation and operating costs; i.e., as pavement deteriorates faster, more frequent rehabilitation is required to maintain a reasonable level of pavement condition; otherwise, vehicles running on poor pavements also suffer from increased consumption of fuel.

We consider for planning purposes temporally homogeneous truck-traffic flow  $f$  on a pavement facility throughout its lifespan (normally 40 to 50 years), measured in average annual daily traffic (AADT). The freight trucks have similar physical dimensions, loading and weight conditions, and performance characteristics (e.g., aerodynamic design, fuel efficiency). The general configuration of a platoon, expressed in terms of relative positions of  $n$  trucks traveling at speed  $v$ , can be defined with the sequences of clearances  $\mathbf{s} = \{s_i\}_{i=1,\dots,n-1}$  and lateral offsets between vehicles  $\mathbf{z} = \{z_i\}_{i=1,\dots,n-1}$ ; see the top part of Figure 1 for an illustration. Each of the aforementioned cost components (i.e., fuel consumption and pavement life cycle costs) for such a platoon of autonomous trucks is evaluated by a series of models in Gungor et al. [9]. These models serve as building blocks of this paper and hence are briefly introduced below.

### TRUCK AERODYNAMICS

When trucks are platooned with small clearances, the head of the trailing truck is under the influence of the wake of the preceding one. Consequently, the incurred air drag force is reduced for both trucks. This phenomenon has been observed in wind tunnel tests [3] and verified in numerical studies [21]. However, there is still a lack of established data, either experimental or simulated, for platooned freight trucks with specified configurations.

Gungor et al. [9] used ANSYS Fluent [22] to conduct computational fluid dynamics (CFD) analysis on the air drag and fuel consumption of platooned trucks. Trucks are modeled in pairs over various combinations of lateral offset  $z$  and clearance  $s$ , and they are exposed to uniform frontal wind at the trucks' cruising speed  $v$ . The (reduced) drag coefficients are obtained from CFD simulations and summarized into a surrogate table of coefficient ratios (i.e., reduced drag coefficient divided by that of isolated trucks). The results, together with field test data [5], are then used through interpolation to compute an air drag correction factor  $R(i|\mathbf{z}, \mathbf{s}, n, v)$  for the  $i^{th}$  truck in the  $n$ -truck platoon. Because the fuel cost for an isolated truck is known [23], the average fuel cost per truck of the platoon can then be estimated by

$$C_{u,drag}(z, s, n|v) = \frac{\alpha_a}{2n} F \rho v^2 D_\infty \sum_{i=1}^n R(i|z, s, n, v)$$

**Figure 1. Equation. Air drag cost function.**

where  $\alpha_a$  is the coefficient translating energy consumption into monetary value;  $F$  is the frontal reference area;  $\rho$  is the density of air; and  $D_\infty$  is the drag coefficient of an isolated truck.

## PAVEMENT DAMAGE AND COST

The traditional and most-used tool for pavement-damage evaluation is MEPDG, which unfortunately has two shortcomings for platooning analysis: It simply assumes a normal distribution of vehicles' lateral wander, and it does not capture the effect of controlled vehicle clearance. To explicitly evaluate the impact of trucks with specific lateral and longitudinal positions, Gungor and Al-Qadi [12] developed a pavement-design framework called Wander 2D. In this model, the strain profile over the pavement's cross section after one truck passing is computed using the finite-element method. The effects of sequential trucks passing that cross section can then be simulated according to the traffic volume (i.e., AADT) to compute the accumulated strain profile. During this process, the influence of longitudinal clearance is also incorporated by correction factors based on the resting-period length  $s/v$  between consecutive trucks (as well as the rest periods between consecutive axial loadings from the same truck). The resultant accumulated strain profile is further used to estimate pavement distress, such as rutting and fatigue cracking. The overall deterioration of pavement at a lateral location  $y$  is measured in terms of the international roughness index  $IRI(y|s, z, n, v, f)$  [12]:

$$IRI(y|s, z, v, f) = IRI_0 + m_1 RD(y|s, z, v, f) + m_2 FC(y|s, z, n, v, f) + m_3 TC + m_4 SF,$$

**Figure 2. Equation. IRI definition.**

where  $IRI_0$  is the initial roughness of a newly constructed pavement;  $RD$  is the rutting depth;  $FC$  is the fatigue cracking;  $TC$  is the thermal cracking;  $SF$  is a site factor; and  $m_1, m_2, m_3, m_4$  are constant coefficients.

In the above,  $RD$  and  $FC$  are computed during the simulation as functions of the accumulated strain;  $SF$  and  $TC$  are independent of the specific traffic-loading features of our interest (i.e., wander and rest period) and thus are treated as constants in our analysis. The key output is the highest IRI value over the entire pavement cross section, denoted by

$$I(s, z, n|f, v) = \max_y IRI(y|s, z, n, v, f),$$

**Figure 3. Equation. Maximum IRI over pavement cross-section.**

which indicates the condition of the most damaged part of the pavement that is likely to fail. Given the relatively even lateral distribution of loading under platooning, the peak pavement damage is

likely to be approximately equal everywhere in the entire pavement cross section. As such, the roughness-development trajectory over time can be computed by the Wander 2D model, assuming that the values of  $RD$  and  $FC$  in (2) are both independent of the lateral location  $y$ . This trajectory also gives the incremental growth of pavement roughness from an initial value of  $I$ , after a certain time period of length  $\tau$  under platooning, denoted by  $\Delta I(s, z, n, I, \tau | f, v)$ . This can be done because the pavement-roughness growth under regular conventional truck traffic is well established in the literature and can be captured by the MEPDG model.

In practice, roughness  $I$  as a comprehensive pavement-distress measure is often used by agencies as the basis for scheduling pavement-rehabilitation activities (e.g., surface mill and overlay up to the damaged depth). For example, when  $I$  reaches a certain threshold, the agency should rehabilitate the pavement segment in order to restore the level of pavement condition. Often, the rehabilitated intensity (e.g., resurfacing thickness) is proportional to the extent of the pavement distress  $I$  (see [24] and [25]); and hence the cost for each rehabilitation activity can be expressed as

$$C_{reh}(I) = aI + b,$$

**Figure 4. Equation. Rehabilitation cost definition.**

where the variable and fixed cost coefficients  $a$  and  $b$  can be estimated using data suggested in the agency's operational guidelines (e.g., [26]).

Another component of the pavement-related life cycle cost captures the user's extra fuel consumption due to the increased rolling resistance and extra vibrations on rougher roads. The vehicle-related user cost  $C_{u,veh}(I|v)$  is computed using a polynomial function, used in [27] and [28] based on the MOVES model ([29], [30]), as follows:

$$C_{u,veh}(I|v) = \alpha_a[I(k_1 + k_2v^2) + k_3v^2 + k_4v + k_5v^{-1} + k_6],$$

**Figure 5. Equation. Vehicle-related cost definition.**

where  $k_1, k_2, k_3, k_4, k_5, k_6$  are constant coefficients. The MOVES model measures all costs in terms of energy per distance, so coefficient  $\alpha_a$  is again used to convert the outcome into monetary cost. The original user-cost formula includes aerodynamic drags with human drivers. To avoid double-counting, we modify  $k_3$  to exclude the component associated with aerodynamic drags. We note that in [27],  $k_3$  is obtained through regression; and it accounts for both the pavement's surface condition (whose effect is a linear function of IRI) and a constant air drag (in the form of  $\rho FD_\infty/2$ ). The influence of air drag can be removed from the above model by subtracting the later constant term from  $k_3$ .

## PRELIMINARY OPTIMIZATION OF PLATOON CONFIGURATION

Gungor et al. [9] explored the possibility of optimizing the lateral offsets and longitudinal clearances for a sequence of trucks (and the associated pavement-rehabilitation schedule), so as to minimize the life cycle cost of the system. Various simplifying assumptions were made, nevertheless. For example,

the traffic consists of platoons whose sizes are limited to be between 2 and 10, as the search spaces grows exponentially with respect to the platoon size. The vehicle speed  $v$  and clearance  $s$  were assumed constant throughout the analysis; pavement rehabilitation was triggered by a fixed threshold whenever  $I$  reached 160 in/mile.

The optimization problem turned out to be a highly nonlinear and non-convex one. It was solved using multiple meta-heuristic methods, including genetic algorithm, pattern-search, and particle swarming; and these methods yielded comparable results. This preliminary effort provided useful insights on how a traffic corridor could potentially be operated under truck platooning, but more general results are needed (e.g., by relaxing the very strong assumptions stated above) so that the results can fit into a network context. This extension will be done in the next section.

## CHAPTER 3: GENERALIZED LINK-COST FUNCTION

In this section, we propose a general framework to optimize the platoon configuration and pavement-rehabilitation schedule simultaneously so as to minimize the total life cycle cost of a dedicated truck-platoon lane under a given homogeneous truck-traffic volume. Vehicle speed  $v$  and link traffic throughput  $f$  continue to be treated as external decisions, the former mainly being driven by safety policies and technological capabilities, while the latter will soon be treated as an endogenous variable in the network model.

### PLATOON CONFIGURATION AND LIFE CYCLE COST

We assume that the lifespan of a dedicated platoon lane is discretized into multiple time periods of duration  $\tau$ , indexed by  $t \in \{1, \dots, T\}$ . Within each period  $t$ , truck traffic of volume  $f$  forms an organized pattern, in which each platoon consists of  $n_t$  perfectly aligned vehicles that are separated by an internal clearance  $s_t$ . Consecutive platoons in the same lane are separated longitudinally by at least a large clearance  $\tilde{s}$  (e.g., 120 ft., which ensures that the platooning effect in aerodynamics or pavement resting is negligible [9]) and displaced laterally by a small offset of  $z_t$ . The platoons collectively form a cyclic pattern, starting from one edge of the lane and rotating back upon reaching the other edge. Such a pattern is desirable because it evenly spreads out the traffic-loading profile over the entire pavement segment (which also provides a large resting period for any cross-sectional location and hence is most favorable for dampening pavement deterioration), while at the same time maximizes fuel savings within each platoon. As such, the platoon configuration in time period  $t$  is defined by three variables  $n_t, z_t, s_t$ , as illustrated in Figure 7. We assume that the highway agency publishes and consistently enforces such a configuration on the dedicated lane within the time period  $t$ .

One of the appealing aspects of platooned traffic is the increased throughput from reduced clearance, as compared to that of human-driven traffic. Consequently, platooning on a separated lane could allow very high flow rate because the speed of platooned trucks (under full automation) can be kept a constant value until the density reaches a physical or regulatory limit (where the speed jumps to 0), which we denote  $Q_1$ . Given the  $f$  and minimum inter-platoon clearance  $\tilde{s}$ , a combination of  $(n_t, s_t)$  is feasible if

$$\frac{f}{24} \leq Q_1 := \frac{n_t v}{\tilde{s} + (n_t - 1)s_t + n_t \times (\text{vehicle length})}.$$

Figure 6. Equation. Link flow capacity.

The lane capacity inferred from this constraint allows quite a high throughput value; for example, if we let  $n_t \rightarrow \infty, s_t = 20$  ft, the upper bound of the allowed flow rate is estimated to be about 4,200 trucks per hour (or AADT = 100,000) at a speed of 60 mph. This value is about four to five times that expected for human-driven truck traffic.

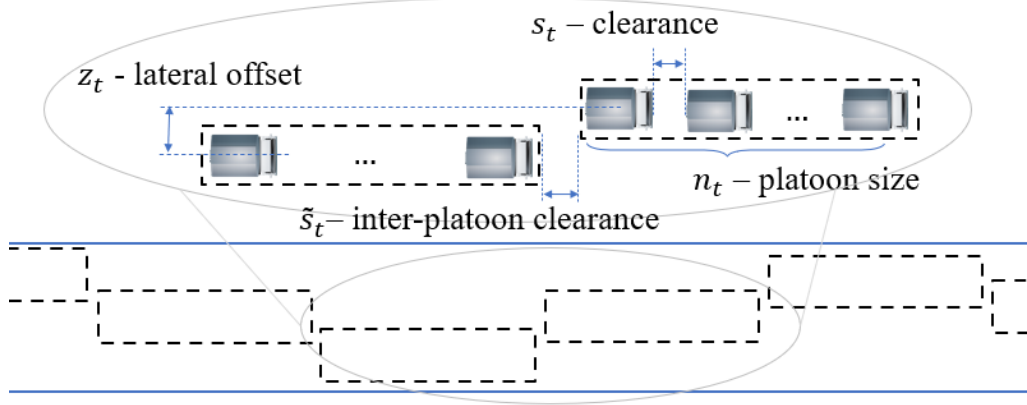


**Figure 7. Diagram. Platoon-configuration definition in a dedicated lane.**

Meanwhile, the agency determines whether to conduct pavement rehabilitation in period  $t$  so as to restore the pavement condition. This decision is denoted by a binary variable  $x_t$ , which equals 1 if resurfacing rehabilitation is scheduled in period  $t$ ; or 0 otherwise. The agency's control variables at period  $t$  then consist of the tuple  $\theta_t = (n_t, z_t, s_t, x_t)$ ; and as a result, the pavement condition at the beginning of period  $t$ , denoted by  $I_t$ , will evolve under the joint influence of all these decisions. Adopting these variables, the life cycle cost components described in Section 2, averaged over the total number of trucks, are hereon written as  $C_{u,drag}(\theta_t|v)$ ,  $C_{reh}(I_t, x_t|f)$ , and  $C_{u,veh}(I_t|f, v)$ , respectively. They satisfy, for all  $t \in \{1, \dots, T\}$ :

$$C_{u,drag}(\theta_t|v) = \frac{\alpha_a}{2n_t} F \rho v^2 D_\infty \sum_i R(i|\theta_t, v),$$

**Figure 8. Equation. Air drag function.**

$$C_{u,veh}(I_t|f, v) = \frac{\alpha_a}{f} [I_t(k_1 + k_2 v^2) + k_3 v^2 + k_4 v + k_5 v^{-1} + k_6],$$

**Figure 9. Equation. Vehicle-related cost function.**

$$C_{reh}(I_t, x_t|f) = \begin{cases} \frac{1}{f} (a I_t + b), & \text{if } x_t = 1 \\ 0, & \text{otherwise} \end{cases}.$$

**Figure 10. Equation. Rehabilitation cost function.**

In addition, whenever (5) holds, the travel speed of the platooned traffic is constant. It translates into a cost per truck-distance of  $\alpha/v$ , if we let  $\alpha$  be the monetary cost associated with one unit of travel time.

The optimal strategy of platoon configuration and pavement-rehabilitation schedule that achieves the lowest life cycle cost (in terms of net present value) is found by solving the following optimization problem:

$$\min_{\{\theta_t\}, \{I_t\}} \sum_{t=1}^T \frac{\alpha}{v} + C_{u,drag}(\theta_t | v) + C_{u,veh}(I_t | f, v) + C_{reh}(I_t, x_t | f) (1+r)^{-t},$$

**Figure 11. Equation. LCC-minimization program over platoon configurations. Objective function.**

subject to Figure 6, Figure 8, and

$$I_1 = I_{min},$$

**Figure 12. Equation. IRI initial condition.**

$$I_t \leq I_{max}, \quad t \in \{1, \dots, T+1\},$$

**Figure 13. Equation. Maximum IRI constraint.**

$$I_{t+1} = \begin{cases} I_{min}, & x_t = 1 \\ I_t + \Delta I(\theta_t, I_t, \tau | f, v), & \text{otherwise} \end{cases} \quad t \in \{1, \dots, T\}$$

**Figure 14. Equation. IRI increment conditional on rehabilitation decision.**

$$x_t \in \{0, 1\}, n_t \in \mathbf{Z}^+, z_t \in [0, z_{max}], s_t \geq s_{min}, \quad t \in \{1, \dots, T\}$$

**Figure 15. Equation. Variable feasible domain definitions.**

In the above,  $r > 0$  is the inflation rate per time period;  $z_{max} > 0$  is the largest allowed lateral displacement (i.e., the width of a lane minus the width of a truck);  $s_{min} > 0$  is the minimum clearance allowed as per safety or regulatory requirements;  $I_{min}$  is the roughness of a new pavement; and  $I_{max}$  is the maximum acceptable roughness for the pavement to be in use. Figure 11 gives the net present value of the life cycle cost. Figure 12 and 13 limit the initial and maximum acceptable pavement conditions; the latter constraint is also enforced at period  $t = T + 1$  so as to avoid quantifying the salvage value of the pavement at the end of the lifespan (which is often controversial and difficult to measure, and a similar treatment can be found in [31] and [24]). Figure 14 states that if a rehabilitation activity is scheduled during a period, pavement roughness is reset to the initial minimum value at the next period; otherwise, it continues to accumulate. Figure 15 defines the value domains of all control variables.

## DYNAMIC PROGRAM SOLUTION

The optimization problem in Section 3.1 is a nonlinear mixed-integer program that includes many highly nonlinear cost components and functions. Practical instances of the problem often involve a large number of time periods, which are hence challenging to solve using conventional algorithms. In this paper, we propose a dynamic programming method to solve the problem. Each time period is naturally chosen as a decision stage. We let  $I_t \in \mathcal{I}$  represent the state of the system at stage  $t$ , where  $\mathcal{I}$  is a discretized arithmetic sequence of roughness values bounded between  $I_{min}$  and  $I_{max}$ . The set of actions at time  $t$  is represented by the variables in  $\theta_t$ .

We define the value function  $V_t(I_t)$  to represent the lowest possible cumulative cost from period  $t$  to period  $T$ , measured as the then-present value while the system is in state  $I_t$  at the beginning of period  $t$ . It should satisfy, for all  $t \in \{1, \dots, T\}$ , the following Bellman equation:

$$V_t(I_t) = \min_{\theta_t} \left[ \frac{\alpha}{v} + V_{t+1}(I_{t+1})(1+r)^{-1} + C_{u,drag}(\theta_t|v) + C_{u,veh}(I_t|f, v) + C_{reh}(I_t, x_t|f) \right],$$

**Figure 16. Equation. Bellman equation.**

subject to Figure 6 to Figure 15; whereas in the final period  $T + 1$ , we set  $V_{T+1}(I_{T+1}) = 0$  as long as the pavement's final condition is ensured by (11). Due to the discretization of roughness values, Figure 14 may have to be approximated; the rounding error will be small when the size of  $\mathcal{I}$  is sufficiently large (e.g., with the bin radius as small as  $\min_{\theta_t} \Delta I(\theta_t, I_{min}, \tau|f, v)/2$ ).

The solution to Figure 16 is found through standard backward recursion. Because the pavement-deterioration process is assumed time-independent in this study, we can enumerate and pre-compute the outcome (and the associated one-stage cost) offline, for implementing each action at each state, and store the minimal one-stage transition cost between states in an  $|\mathcal{I}|$ -by- $|\mathcal{I}|$  matrix. At the end of the recursion, the optimal net present value of the life cycle cost at period 1 is given by  $V_1(I_{min})$ . Then a standard backtracking of the optimal state-transition path can then be conducted forward in time to recover the set of optimal actions in all the stages.

The above modeling framework can be used by the agency to obtain optimal life cycle cost per vehicle-distance under any given flow volume  $f$ . This process can be repeated for a set of traffic flow volumes to yield the link-cost function for dedicated truck-platoon lanes. The resulting optimal cost components, as functions of  $f$ , are denoted as  $\tilde{C}^{reh}(f)$ ,  $\tilde{C}^{veh}(f)$ , and  $\tilde{C}^{drag}(f)$ .

Among the cost components, the reductions of  $\tilde{C}^{reh}(f)$ ,  $\tilde{C}^{veh}(f)$ , and  $\tilde{C}^{drag}(f)$  from platooning are normally borne by the users, while the associated increase in pavement construction and rehabilitation cost is normally borne by the agency. Here, we assume that the agency is willing to explore pricing policy instruments (e.g., a fixed user fee per truck-mile. The idea is similar to the current overweight-vehicle permit program that is implemented in many states in the United States [32]) to transfer some of the rehabilitation and construction costs of the platoon lane to the users. This decision is considered next as part of an integrated model that designs a network of dedicated truck-platoon lanes.

# CHAPTER 4: NETWORK DESIGN

## BI-LEVEL MODEL

Like many other transportation-planning problems, the system of interest involves at least two decision-makers: (i) the highway agency, in charge of planning the physical roadway infrastructure and operational rules, which determines placement of the platoon lanes, the platoon configuration, and pavement-rehabilitation decisions over time, as well as the user fees so as to minimize the life cycle costs; (ii) freight carriers and shippers, informed with the platooning options and regulations, who will then decide for themselves the routes to take and whether to use truck-platoon lanes in order to minimize their individual travel costs. Therefore, it is natural to formulate this problem as a bi-level network-design and traffic-equilibrium model.

Consider an existing highway network consisting of a set of directed arcs  $A$  and a set of nodes  $N$ , serving time-invariant truck-traffic demand associated with a set of OD pairs  $\{q^{od}: o, d \in N\}$ . Let  $D_{ij}$  be the length of arc  $(i, j) \in A$ ,  $Q_0$  the capacity of a regular lane, and  $l_{ij}$  the number of existing lanes in arc  $(i, j)$ .

We first consider the upper-level model, where the highway agency identifies a subset of the highway arcs  $A_1 \subseteq A$  that can technically be considered as candidates for installing dedicated platoon lanes. The set of other arcs are denoted  $A_0 = A \setminus A_1$ . We use binary variable  $\delta_{ij}$  to denote the lane-conversion decision, which takes value 1 if one of the regular lanes on arc  $(i, j) \setminus A_1$  is selected for conversion into a platoon lane; or 0 otherwise. In light of the high capacity of dedicated platoon lanes as indicated by Figure 6, we do not consider converting more than one lane per arc. However, from a modeling point of view, this assumption could be relaxed; variable  $\delta_{ij}$  could take an integer value that represents the actual number of converted lanes. In addition, the platoon lane could also be added to an arc (e.g., in the median or shoulder). In this paper, however, we consider only the option of converting at most one existing highway lane, so as to stay focused. We assume the construction cost for conversion is  $\alpha_d$  per lane-distance. The vector  $\delta = \{\delta_{ij}\}_{\forall (i,j) \in A_1}$  then defines the subset of highway network arcs that experience lane conversion. All other regular lanes are assumed to operate regularly with non-platooned traffic. We assume that all trucks are capable of switching between platooning and non-platooning operations freely. As per safety regulations for mixed traffic (e.g., that involving vehicles with level 3 automation or below), every truck must have a human driver in order to drive normally on regular lanes; but it yields control and follows the centrally broadcast configurations in platoon lanes.

To distinguish between regular and platoon lanes, we hereby use subscript  $p \in \{0,1\}$  in  $\tilde{C}_p^{reh}(f)$ ,  $\tilde{C}_p^{veh}(f)$ , and  $\tilde{C}_p^{drag}(f)$  to indicate the respective minimum link-cost components, where  $p = 1$  for those evaluated with the optimal platooning strategy; and  $p = 0$  for those evaluated as regular traffic. For the latter, each truck is treated as being in isolation while computing the fuel consumption from air drag; the pavement deterioration is accumulated assuming the trucks' wander follows a default normal distribution per the MEPDG manual [33], and the effect of resting period is ignored (i.e., not adjusted by a factor); the pavement is rehabilitated whenever the roughness index

reaches 160 (in/mi). The link congestion cost per truck-distance in a platoon lane, again, is simply denoted  $C_1^{cong}(f) = \frac{\alpha}{v}$  as long as Figure 6 holds; for a regular lane, the counterpart, denoted  $C_0^{cong}(f)$ , is a function of traffic flow. The form of this function can be adopted from the literature, e.g., the standard form of BPR function [34]:

$$C_0^{cong}(f) = \frac{\alpha}{v} (1 + \beta_1) \left[ \frac{f}{(l_{ij} - \delta_{ij}) Q_0} \right]^{\beta_2}, \forall (i, j) \in A,$$

**Figure 17. Equation. Travel time cost function.**

where  $\beta_1$  and  $\beta_2$  are constant parameters that capture the congestion effect.

Once the platoon lanes are placed in the highway network, the freight carriers will attempt to route their fleets and use the platoon options accordingly. Most often, there is a large number of carriers; and they aim at minimizing their own costs via a traffic-assignment problem in the lower level. These carriers, categorized by superscript  $od$ , collectively decide the truck traffic that traverses each network link and whether to split that traffic through regular or platoon lanes (whenever applicable).

We denote the set of arc-lane traffic flow by  $f = \{f_{ij,p}^{od}\}_{\forall p, od, (i,j)}$ , where  $f_{ij,p}^{od}$  is the amount of truck flow from origin  $o$  to destination  $d$  on type- $p$  lane(s) of arc  $(i, j) \in A$ . As such, the total flow in the type- $p$  lane(s) can be expressed as

$$v_{ij,p} = \sum_{od} f_{ij,p}^{od}, \quad \forall p, (i, j) \in A.$$

**Figure 18. Equation. Total link flow definition.**

Because truck platooning accelerates pavement deterioration and increases agency cost, we consider redistributing a portion of the agency's cost to the users. In practice, such a compensation is usually imposed through tolls upon using the dedicated platoon lanes (similar to tollway fees or overweight-truck permit fees). We consider the toll, denoted as  $W$ , as a fixed price per truck-distance imposed on the dedicated platoon lanes.

The bi-level model can be formulated as follows:

$$\min_{\delta, W} \sum_{(i,j) \in A} D_{ij} \left\{ \alpha_d \delta_{ij} + \sum_{p \in \{0,1\}} v_{ij,p} \left[ \tilde{C}_p^{reh}(v_{ij,p}) + \tilde{C}_p^{veh}(v_{ij,p}) + \tilde{C}_p^{drag}(v_{ij,p}) + C_p^{cong}(v_{ij,p}) \right] \right\}$$

**Figure 19. Equation. Upper-level objective function.**

subject to Figure 17, and

$$\delta_{ij} \in \{0,1\} \forall (i,j) \in A_1, W \geq 0$$

**Figure 20. Equation. Upper-level variable domain definition.**

where  $f$  solves

$$\min_f \sum_{(i,j) \in A} \int_0^{v_{ij,p}} \left[ \tilde{C}_p^{veh}(w) + \tilde{C}_p^{drag}(w) + C_p^{cong}(w) + pW \right] dw$$

**Figure 21. Equation. Lower-level objective function.**

subject to

$$\sum_{(j,i) \in A} \sum_{p \in \{0,1\}} f_{ji,p}^{od} - \sum_{(i,j) \in A} \sum_{p \in \{0,1\}} f_{ij,p}^{od} = \begin{cases} -q^{od}, & i = o \\ \text{otherwise}, & \forall o, d, i \in N, \\ q^{od}, & i = d \end{cases}$$

**Figure 22. Equation. Flow conservation constraint.**

$$f_{ji,1}^{od} \leq 24Q_1 \delta_{ij}, \forall o, d \in N, (i,j) \in A_1,$$

**Figure 23. Equation. Link flow capacity constraint.**

$$f_{ij,1}^{od} = 0, \forall o, d \in N, (i,j) \in A_0,$$

**Figure 24. Equation. Infeasible link flow constraint.**

$$0 \leq f_{ji,p}^{od} \leq 24Q_p, \forall o, d \in N, p \in \{0,1\}, (i,j) \in A,$$

**Figure 25. Equation. Lower-level variable domain definition.**

Figure 18 gives the objective function for the upper-level model, minimizing the societal disutility as the sum of all user and agency costs on all network lanes; Figures 19 indicate the domain of the upper-level variables. Lower-level objective function Figure 20 stipulates that the traffic flow reaches user equilibrium, as the carriers are mainly concerned with their individual time and out-of-pocket costs, including fuel consumption (attributed to both air drag and rolling resistance), congestion, and the toll fee; Figure 21 ensures flow conservation, and Figures 22 and 23 allow truck-platoon traffic only when a link contains a dedicated platoon lane; Figure 24 states the range of feasible flow values.

## SOLUTION METHOD

We first consider the solution approach to the lower-level network flow model. Because the objective function Figure 20 is clearly non-convex (and may not even be nondecreasing), we do not have theoretical proofs for existence or uniqueness of the solution. However, our experiments show that the solution approaches established for convex or concave link-cost functions ([35], [36]) can be applicable to small- to medium-size problems. In this study, we use the standard Frank-Wolfe [37] algorithm. At each iteration, the step size is determined by a local backtracking line-search [38]. The algorithm is terminated at convergence or when a fixed maximum iteration number is reached.

The solution algorithm for the lower-level problem serves as a sub-module to determines the optimal values of network design  $\delta$  and platoon-lane fee  $W$  at the upper level. Conditional on any value of  $W$ , we use a simple meta-heuristic method, the simulated-annealing algorithm [39], to solve the network-design problem. Finally, we use a golden-section search to determine the optimal fee value  $W$ .

While implementing the simulated annealing algorithm, the initial network design  $\delta$  can be generated randomly; a solution can be perturbed by flipping and swapping elements of this vector. The annealing temperature can be initially comparable to the expected upper-level objective value, and its value is subsequently decreased by a fixed multiplicative factor after certain number of iterations.

## CHAPTER 5: NUMERICAL RESULT

In this section, we apply the models in Sections 3 and 4 to realistic examples to demonstrate their applicability, and also to draw insights. The models and algorithms in the link-level are coded in MATLAB (to utilize the tools developed in [19]), and those in the network-level are coded in Python; and all run on a personal computer with 3.1 GHz CPU and 8GB RAM.

### OPTIMAL PLATOON AND LINK-COST FUNCTION

In this section, we first use the dynamic programming framework from Section 3 to optimize the platoon configuration, as well as the rehabilitation schedule, to establish the generalized link-cost function. The truck traffic consists of identical class-8 trucks weighing 80 kips (35.7 tons) each, and the predetermined free-flow travel speed (with or without platooning) is 60 miles per hour. The planning horizon is assumed to be 45 years, and the time period  $\tau$  is assumed to be half a year. Hence, we have  $T = 90$ . The monetary discount rate per period is  $r = 1.5\%$ , equivalent to a 3.02% annual interest rate. We consider that the pavement is composed of a 12-in asphalt concrete layer over a 12-in base layer, and the mechanical parameters (e.g., elastic modulus) are the same as those used in [28]. According to AASHTO [33], coefficients  $m_1$  to  $m_4$  in Figure 2 equal 40 (1/mi), 0.4 (in/mi), 0.008 (in/ft), and 0.015 (in/mi), respectively. According to [40], performing milling and overlay would fully recover the pavement condition from the worst acceptable level  $I_{max} = 160$  (in/mi) to the new level  $I_{min} = 60$  (in/mi), at a cost of  $1.5 \times 10^6$  \$/mi-lane. We assume half of that cost is fixed (e.g., labor and machinery) and half is variable (e.g., material and energy), and choose  $a = 7.5 \times 10^3$  \$/in-lane,  $b = 7.5 \times 10^5$  \$/mi-lane. Following [41], the coefficients  $k_1$  to  $k_6$  in Figure 5 take values  $1.36 \times 10^{-4}$  (kJ/in),  $1.4$  (kJ·hr<sup>2</sup>/in·mi<sup>2</sup>),  $-3.59 \times 10^{-1}$ (kJ·hr<sup>2</sup>/mi<sup>3</sup>),  $-2.65 \times 10^2$ (kJ·hr/mi<sup>2</sup>),  $8.28 \times 10^4$ (kJ/hr), and  $1.92 \times 10^4$ (kJ/mi), respectively.

In evaluating the energy consumption due to air drag, we pick  $\rho = 0.081$  lb/ft<sup>3</sup>,  $F = 102.1$  ft<sup>2</sup>. The energy-cost coefficient is  $\alpha_a = 3.96 \times 10^{-5}$  \$/ft-lb (or  $2.92 \times 10^{-2}$  \$/kJ). According to the *Highway Capacity Manual* [42], the coefficients in the BPR function for heavy-duty trucks are chosen as  $\beta_1 = 0.25$ ,  $\beta_2 = 9.0$ , and the regular lane traffic-flow capacity  $Q_0 = 880$  per hour per lane. Here, we conservatively assume that a driver is still needed even if a truck is autonomous, so as to allow it to travel safely on regular lanes and to ensure safety against emergencies. The monetary value of travel time is assumed to be  $\alpha = 52$  \$/hour, including 30 \$/hour for driver wage and benefits, and 22 \$/hour for vehicle depreciation [43].

We apply the dynamic program algorithm to evaluate the minimum generalized cost for a range of AADT values  $f = \{20, 2 \times 10^4, 4 \times 10^4, \dots, 1 \times 10^5\}$ . For computational convenience, the platoon-configuration variables are assumed to take values from the following discretized sets:  $n_t \in \{2, 5, 10, 15, 20\}$ ,  $z_t \in \{0, 0.1, 0.2, 0.3, 0.4\}$  ft, and  $s_t \in \{20, 30, 40, 50, 60\}$  ft.

Figure 26 shows the optimal pavement-deterioration process and rehabilitation schedule (indicated by  $I$ ) over the planning horizon, as well as the associated optimal platoon configurations, when the dedicated platoon lane serves truck-traffic AADT of 40,000 and 100,000. In the top figure, both IRI trajectories exhibit a clear cyclic pattern, with a constant trigger value for rehabilitation that is

reached at regular intervals (i.e., every 25 and 10 years, respectively) until the end of the planning horizon. This overall pattern is consistent with the findings from theoretical analysis in [31]. Although the piecewise linearity of the trajectories should be largely caused by the discretization of IRI value levels in the dynamic programming model, it nevertheless shows a clear concave IRI accumulation curve during each post-rehabilitation interval—including a brief period of rapid roughness deterioration first (e.g., for 2 to 3 years), followed by a slower IRI increase process throughout the rest of the interval. This concave IRI accumulation trajectory may be surprising, but it can be attributed to the time needed for new asphalt concrete pavement to harden (i.e., the first few years after rehabilitation). Pavement hardening stiffens and embrittles the pavement and makes it easier to crack but more resistant to rutting [44]. In contrast, the semi-channelized loading pattern brought by platooned traffic would damage the pavement mostly in the form of rutting. Consequently, in the later part of the rehabilitation cycle, the pavement-deterioration process typically slows down. Similar findings have been reported in [28] and [45].

The cyclic pattern of the IRI trajectories is well matched with the associated platoon configuration, as shown in the mid and bottom parts of Figure 26. Apparently, the dynamic program takes into account the rapid vs. slow deterioration processes, and chooses to use smaller platoons with larger clearances during the fast-deterioration part of the post-rehabilitation interval (i.e., temporarily favoring pavement preservation over air drag), and then later uses larger and more compact platoons to achieve air drag reduction. The lateral shift  $z_t$ , in contrast, does not impact the air drag due to the perfectly aligned platoon in this study. It affects only pavement deterioration and thus, for both cases, takes the same optimal value (the smallest nonzero value) that contributes the least to pavement deterioration.

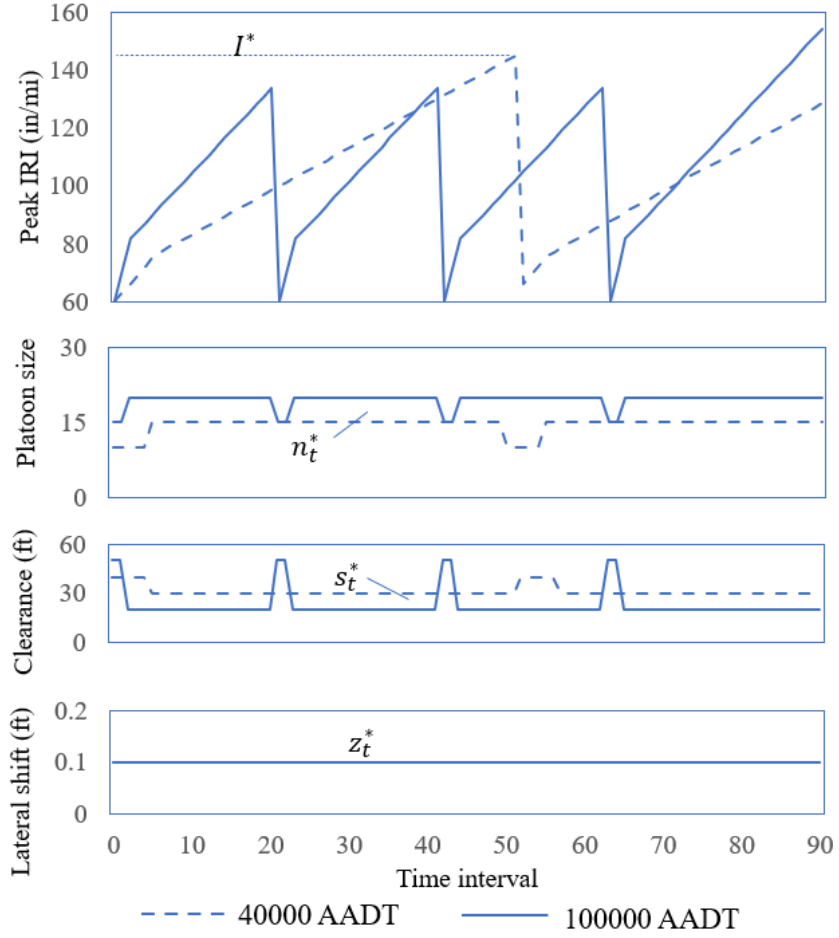


**Figure 26. Graph. Optimal platoon configuration and rehabilitation schedule over the planning horizon for AADT = 40,000 and 100,000.**

We notice that the optimal truck-platoon configuration is largely constant in the post-hardening parts of the post-rehabilitation intervals (which collectively cover over 90% of the entire planning horizon). Hence, for convenience, policy-makers may simply use these dominating platoon configurations, labeled as  $n_t^*$ ,  $s_t^*$ , and  $z_t^*$  in Figure 26, throughout the entire planning horizon; and correspondingly, rehabilitation can be conducted whenever the pavement roughness reaches the constant triggering threshold, which is labeled as  $I^*$ . These representative control variables for a range of traffic-flow levels are listed in Table 1. The pavement-rehabilitation trigger value decreases slightly as traffic volume increases, while the platoon size varies between 15 and 20 trucks, and the clearance varies between 20 and 40 feet.

**Table 1. Representative Platoon Configurations and Pavement-Rehabilitation Thresholds**

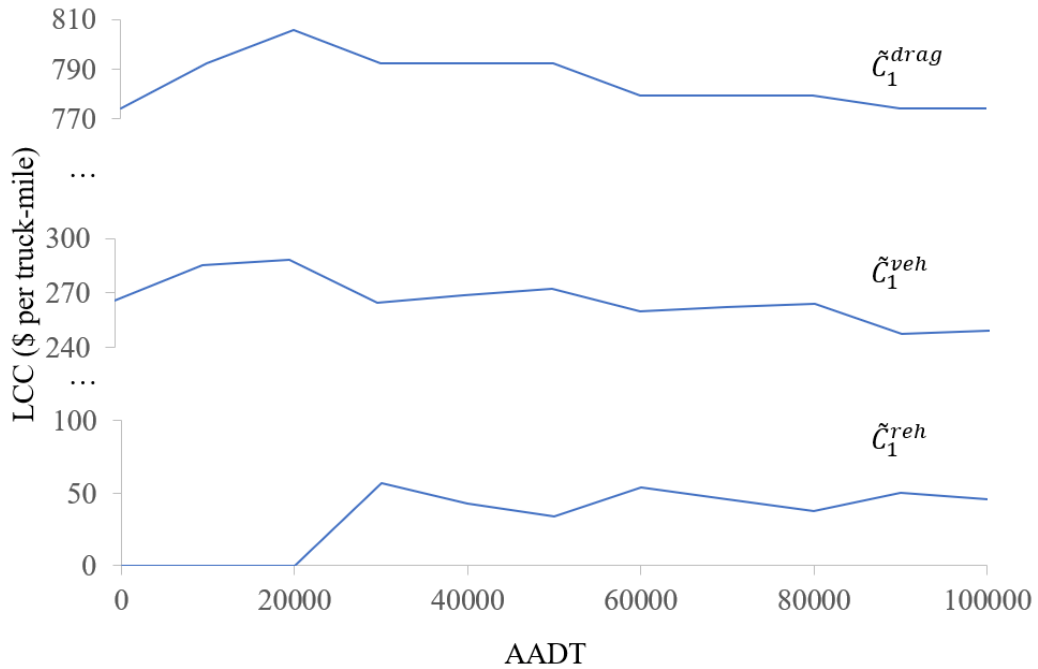
AADT	$I^*$ (in./mi.)	$n_t^*$	$s_t^*$ (ft.)	$z_t^*$ (ft.)
20 (very low traffic)	160.0	20	20	0.1
20,000	160.0	15	40	0.1
40,000	145.6	15	30	0.1
60,000	142.1	15	20	0.1
80,000	138.3	15	20	0.1
100,000	135.4	20	20	0.1

Figure 27 shows the optimal cost components per truck-mile in the platoon lane, including the user costs due to air drag and rolling resistance, and the agency cost for rehabilitation, under optimized platoon configuration and rehabilitation schedule, as functions of AADT.

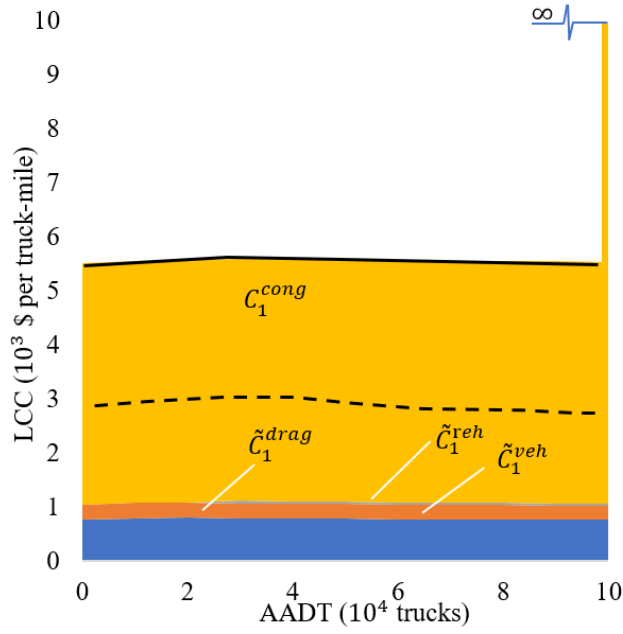
From the figure, we can see that the cost due to air drag is dominating among the three—possibly due to the relatively high free-flow speed at which air drag is significant. With our parameters, there is almost no need to rehabilitate the pavement in the entire planning horizon under very low traffic (for AADT ranging from 20 to 20,000). Meanwhile, as traffic increases within this low range, the user-cost components both increase, through varying platoon configurations, in order to compensate for the accelerated pavement deterioration. After AADT exceeds 20,000, pavement rehabilitation starts to occur; and the user-cost components (per truck-mile) decrease accordingly. These results are consistent with the information from Figure 26 and Table 1. Because the rehabilitation cost is almost an order of magnitude smaller than the other cost components, and the pavement deteriorates at a constant rate regardless of the frequency of rehabilitation, under heavy traffic, overall cost savings can be improved by rehabilitating pavement more frequently and even further by using larger and more compact truck platoons. In this study, we have assumed that the rehabilitation activities fully renew the pavement, after which the roughness accumulates as if the pavement were newly constructed. This simplification may lead to underestimation of pavement deterioration under heavy traffic.

Finally, Figure 28a plots the total link cost per truck-mile in a platoon lane, including the above-mentioned components, as well as the travel-time cost. Despite small fluctuations as discussed above, the curve is relatively flat. For AADT larger than 100,000, Figure 6 is violated; and hence the cost goes to infinity. We also notice that the travel-time cost dominates all other cost components, partly due to our conservative inclusion of travel-time cost due to human drivers. This observation brings in another appealing incentive for freight carriers, as technologies for truck platooning continue to advance, to reduce or even eliminate the deployment of human drivers—this reduces not only the direct driver cost but also the societal cost associated with potential fatalities in crashes. To examine the effect of this possibility, we additionally consider a scenario where the payment for the driver is completely eliminated from the monetary cost of travel time (i.e.,  $\alpha = 22$  \$/hour) whenever truck driving is automated in a platoon lane. As such, drivers are assumed to be able to alight/board the trucks at the beginning/end of the platoon lanes without extra cost. In this case, the new life cycle cost (LCC) function is shown as the black dashed line in Figure 28a.

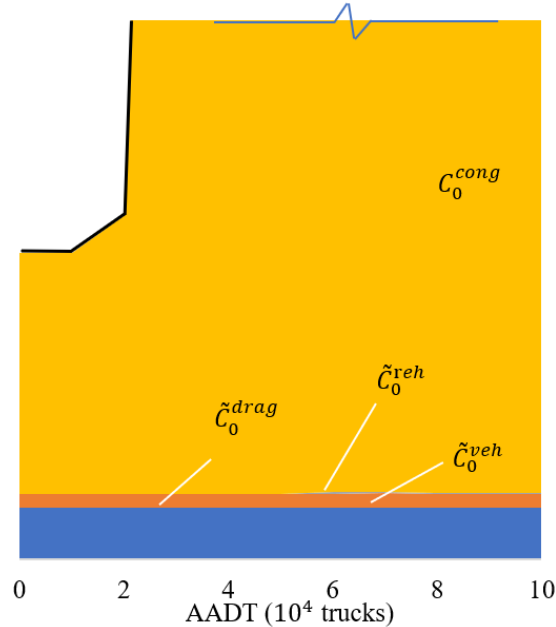
For comparison, Figure 28b shows the counterpart cost per truck-mile for a regular lane. The cost due to air drag is constant and larger, the cost related to vehicle operations is slightly smaller, and that for pavement rehabilitation is almost negligible, mainly due to random truck wander and much slower pavement deterioration with human drivers. The major difference is the travel-time cost due to the presence of heavy congestion in the regular lane, which increases rapidly when traffic flow approaches its capacity (around 21,000 AADT). For human drivers, there is a similar safety limit of about 25,000 AADT if we assume a minimum clearance of 240 ft and truck length of 55 ft. In this example, however, we ignore this safety requirement for regular traffic because this feasibility constraint is implicitly enforced by the very high congestion cost at such high values of traffic flow.



**Figure 27. Graph. Link-cost components for platooned truck traffic.**



(a) Platoon lane.



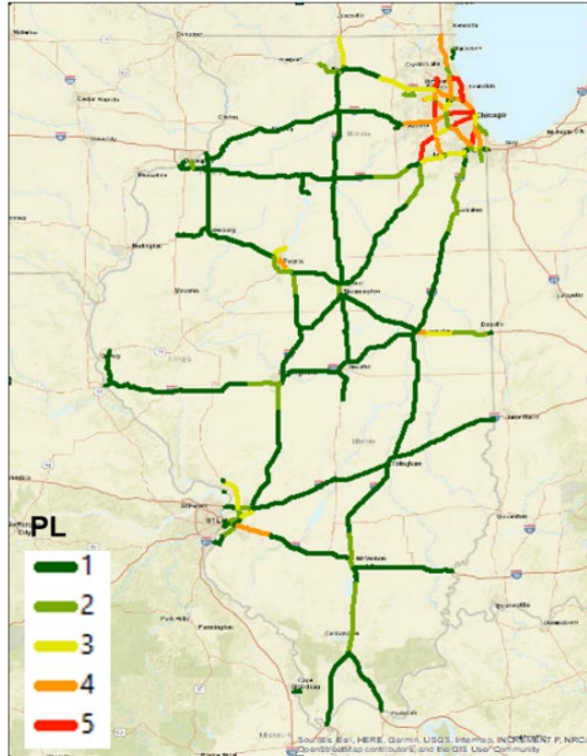
(b) regular lane.

**Figure 28. Graph. Link-cost function.**

## NETWORK-LEVEL OPTIMIZATION

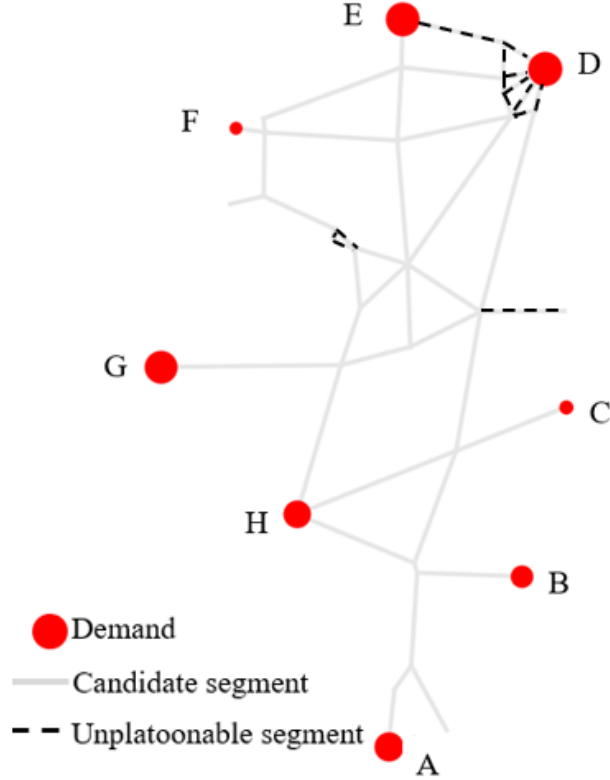
We now apply the bi-level model from Section 4 to the freeway network in the state of Illinois. The existing roadway segments that are suitable for conversion to platoon lanes have recently been

identified by in [46], based on the traffic capacity and the expected amount of vehicle interactions (e.g., lane changing, passing). The map of the freeway network is shown in Figure 29a, together with its abstraction in Figure 29b. The arcs in  $A_1$  are shown as grey solid lines, and those in  $A_0$  are shown as black dashed lines. For simplicity, we let  $l_{ij} = 2, \forall (i,j) \in A$ , in this case study.



(E. Okte, I.L. Al-Qadi, 2020)

(a) Freeway segments suitable for platooning. (source: [46]);



(b) network abstraction and OD nodes.

**Figure 29. Diagram. The Illinois network.**

Truck-traffic demand data are extracted from the Illinois Roadway Information System database, which stores measured truck-traffic data at a selection of weigh-in-motion (WIM) sites along main interstate freeway corridors. Although the current traffic demand is rather low, we believe that the truck traffic will increase significantly as autonomous trucks become prevalent. Hence, in the following numerical experiments, we scale the traffic demand up by at most an order of magnitude from the current traffic levels. Based on the data, eight major demand points (each with a large traffic volume) with a reasonable spatial dispersion are selected as the traffic origins and destinations. They are illustrated by the red markers in Figure 29b, whose size roughly represents the total incoming and outgoing traffic volumes. The inflow or outflow of each point equals the measured traffic in a suitable direction (e.g., for location A, the north-bound traffic is assumed to have originated from A; and the south-bound traffic is assumed to be destined toward A). In computing the OD matrix, we assume that demand from any origin is simply distributed proportionally to all destinations based on these destinations' measured total incoming demand. In the following discussions, we indicate the demand level by the total daily traffic demand in the network  $\sum_{od} q^{od}$ . The resultant demand matrix, where  $\sum_{od} q^{od} \approx 1 \times 10^5$ , is shown in Table 2.

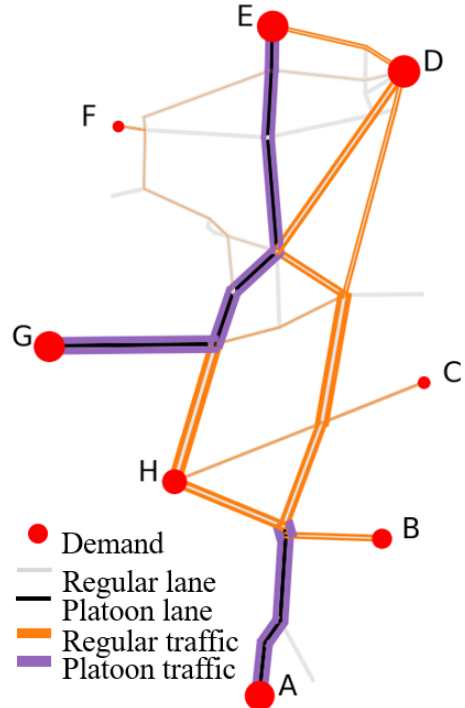
**Table 2. Origin–destination demand matrix in AADT (scaled from 2012 WIM data)**

	A	B	C	D	E	F	G	H
A	0	1167	401	3389	5966	333	4572	1844
B	1097	0	202	896	1644	168	2251	948
C	361	193	0	561	541	55	494	312
D	3367	153	675	0	5494	561	8015	3049
E	6204	1876	645	5448	0	536	2693	4529
F	299	160	55	465	448	0	409	258
G	4729	2430	578	7881	2004	480	0	1363
H	1850	990	340	3026	4272	283	1180	0

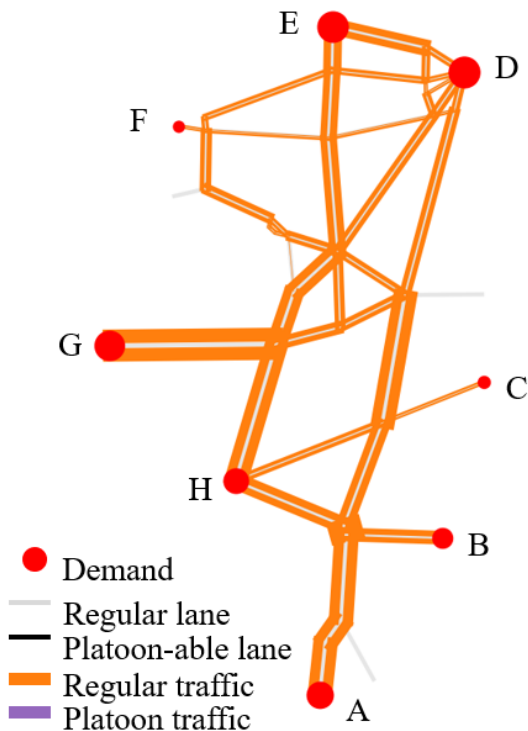
As such, this example network consists of 35 nodes, 104 directed arcs, and 56 demand OD-pairs. In applying the simulated annealing algorithm, we initialize the temperature as 10% of the objective cost under a simple benchmark solution (i.e., where no lanes are converted) and multiply it by a factor of 0.8 every 20 iterations. The golden-section search for  $W$  is initiated within the interval  $[0,0.5]$  (\$ per truck-mile) to enclose some commonly chosen values [43]. The solution to the network-design model converges within 400 iterations, and the traffic-assignment subroutine normally converges within 50 iterations. A moderate value of tolerance (within 1% to 3% of the initial objective value) is used for the traffic-assignment model because sometimes the equilibrium may not be unique. Overall, solving one instance of the bi-level model for our network takes around 2.5 hours.

For the baseline case (noted as case 1), we select  $\alpha_d = 4 \times 10^6$  \$/lane-mile and  $\sum_{od} q^{od} \approx 1 \times 10^5$ . Figure 30a shows the optimal network design for platoon lanes (shown as solid black lines), as well as the equilibrium truck-flow pattern in both types of lanes (shown as the two types of colored thick lines, where thickness is proportional to flow volume). The optimal toll price in this case is 0.116 (\$/truck-mile). Under this network design, the average life cycle cost for one truck trip in the present value is 156.6 (\$/truck-trip). As shown in the figure, a set of network arcs (24.7% of the total network lane-miles), mostly those expected to carry large flow, are chosen for lane conversion. These platoon lanes themselves form two main corridors connecting some of the major demand points. If both platoon lane and regular lane are present in a network arc, truck traffic would always prefer using the platoon lane (due to the relatively lower link cost, as shown in Figure 28) until its capacity  $Q_1$  is reached. This case could represent the early stage of implementing the truck-platooning system, where the conversion cost is still high and the demand has yet to ramp up, such that the limited placement of platoon lanes is concentrated in regions with high traffic demand (e.g., E-G-H).

For comparison, Figure 30b shows the equilibrium flow pattern under the benchmark solution, where there is no lane conversion, and the same demand. We call this solution benchmark 1. The flow distribution is much more even across the network, probably due to the much faster increase of travel-time cost in congested regular lanes. By comparing these two figures, it is clear that the dedicated platoon lanes play a significant role in concentrating traffic from peripheral parts of the network into a few major corridors (where dedicated lanes are available). The average life cycle cost for one truck trip in this benchmark is 179.3 (\$/truck-trip), and hence implementing the proposed network design in Figure 30a would reduce the total life cycle cost by 14.4%.



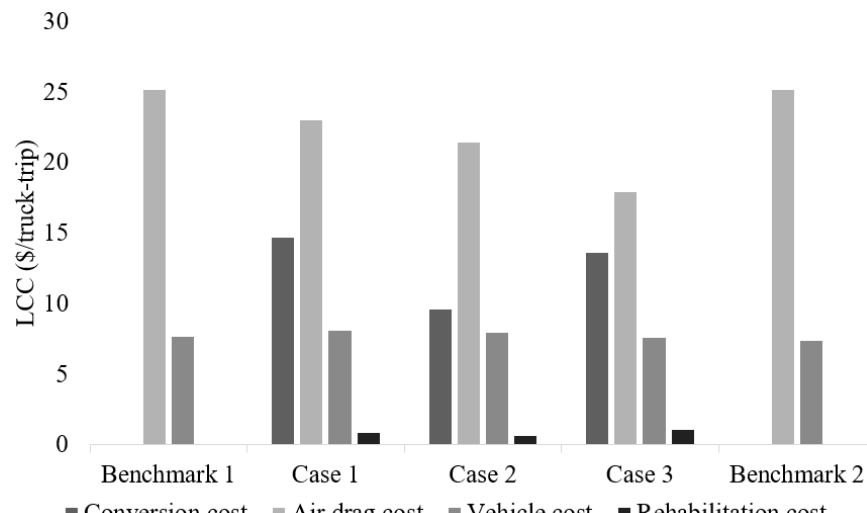
(a) Baseline case 1:  $\alpha_d = 4 \times 10^6$ .



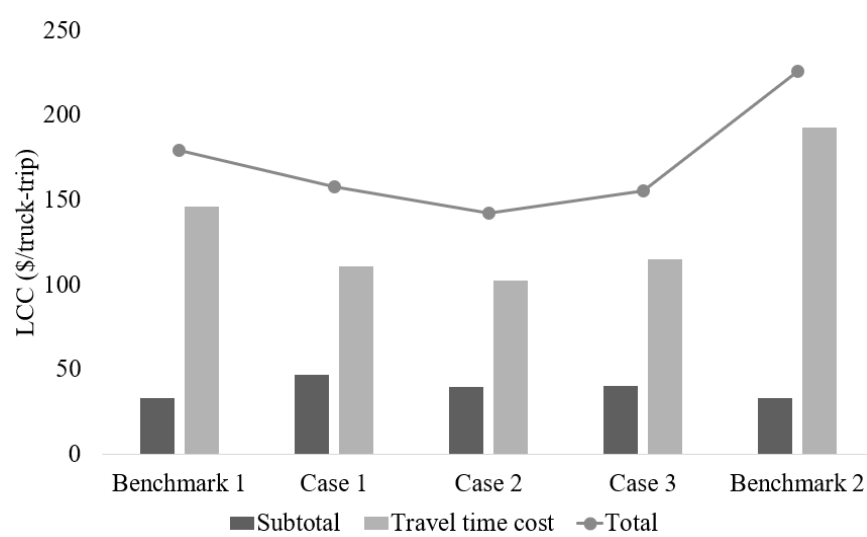
(b) Benchmark 1 (no platoon lanes).

**Figure 30. Diagram. Network design and flow pattern.**

Figure 31a further breaks down the cost components, including fuel costs, vehicle-operation cost, rehabilitation cost, and lane-mile conversion cost for these solutions. Figure 31b plots the total LCC, now including the travel-time cost; the cost components shown in Figure 31a are now summed into a subtotal. The left two groups of these figures show the cost comparison for case 1 and benchmark 1. The differences in vehicle cost appears minimal because the increased pavement deterioration is mainly soaked by rehabilitation cost, which is of smaller magnitude and optimized in the link-level platoon configuration model. In contrast, with certain investment in converting lanes for platooning, a significant reduction can be achieved in the users' air drag and travel-time costs (14.4% and 25%, respectively). The latter, particularly, may be very appealing to the transportation agency because it is achieved with a very small amount of investment.



(a)



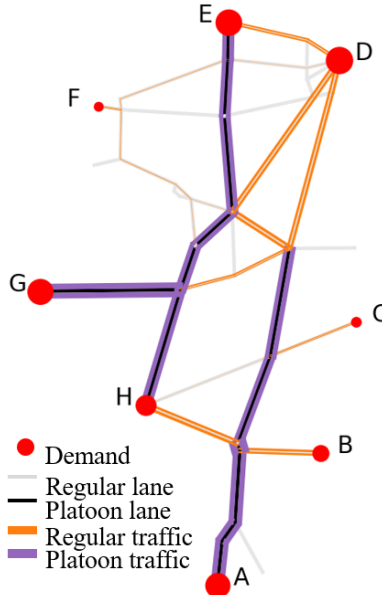
(b)

**Figure 31. Graph. Life cycle cost components breakdown for five cases.**

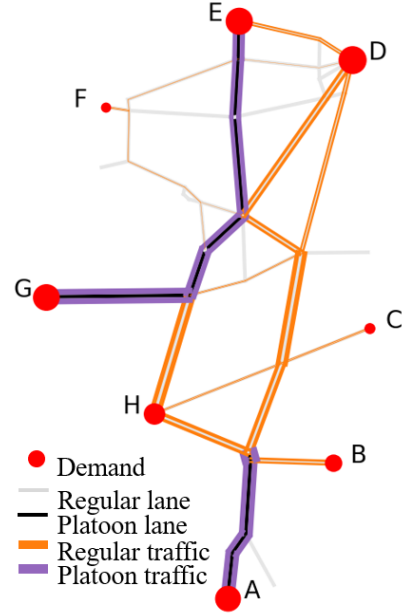
For additional comparison, Figures 32a and 32b show two additional optimal network designs and traffic-flow patterns. When  $\alpha_d$  reduces to  $2 \times 10^6$  (which we note as case 2), its network design is shown in Figure 32a. The optimal toll price is 0.127 (\$/truck-mile); the optimal lane-mile conversion percentage and the corresponding cost saving from lane conversion (as compared to the cost under benchmark 1) are 36.25% and 21.56%, respectively. The increases in both improvement percentages are not surprising. As compared to Figure 30a, this solution has more converted lanes on which more traffic may enjoy the benefit from reduced air drag and travel time.

In contrast, when the demand increases to a higher level,  $\sum_{od} q^{od} \approx 2 \times 10^5$ , while the conversion cost remains high at  $\alpha_d = 4 \times 10^6$ , the model result is plotted in Figure 32b. We note this as case 3. The toll price for this scenario is 0.119 (\$/truck-mile), and the cost savings from optimal lane conversion is as high as 42.51%—again, as compared to the corresponding no-platoon-lane design under the same high demand (which is noted as benchmark 2 and plotted in Figure 32c). In case 3, the traffic demand is approaching the capacity of regular lanes on certain arcs. Consequently, a notable set of arcs (45.76% of the lane-miles) is converted, which almost forms a complete platoon lane network that connects all demand points. The platoon lanes effectively pool and concentrate the truck traffic in the network.

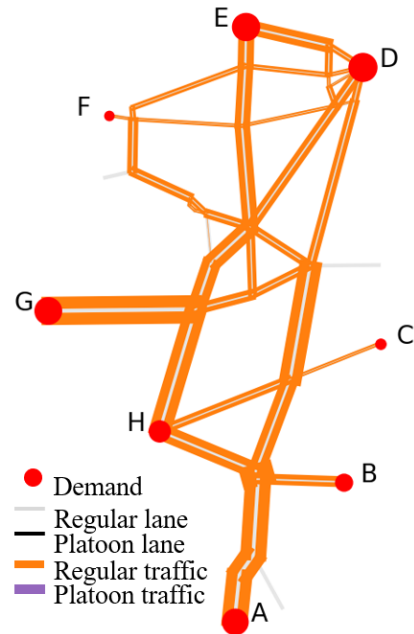
The three groups on the right-hand side of Figure 31 show the life cycle cost components for cases 2 and 3, as well as benchmark 2. The pattern is consistent with the other two groups. By comparing case 2 with case 1, we see how the lower lane-conversion cost would encourage more lanes to be converted so as to reduce the user-cost components (both fuel and travel time). As the traffic demand increases (i.e., from case 1 to case 3), traffic congestion throughout the network is escalated; but the conversion cost may be borne by more trucks as well (due to gain of economies of scale). Consequently, the converted lane-mile is further increased; and it is highly favorable to convert most of the busy corridors that can pool more demand and bring benefits to a larger portion of the traffic.



(a) Case 2:  $\alpha_d = 2 \times 10^6$  (\$/lane-mile) and  $\sum_{od} q^{od} \approx 1 \times 10^5$  AADT.



(b) Case 3:  $\alpha_d = 4 \times 10^6$  (\$/lane-mile) and  $\sum_{od} q^{od} \approx 2 \times 10^5$  AADT.



(C) Benchmark 2(no platoon lanes,  $\sum_{od} q^{od} \approx 2 \times 10^5$  AADT.

**Figure 32. Graph. Network design and flow pattern.**

The discussion of Figures 30 to 32 highlights the significant impacts of lane-conversion cost rate  $\alpha_d$  on the network design. Yet, the material and structural design of smart and connected infrastructure for truck platooning is still under development; and there is currently no good way to estimate its value.

Hence, we conduct a sensitivity analysis to see how the value of  $\alpha_d$  impacts the optimal network design and system performance. We set a lighter traffic demand,  $\sum_{od} q^{od} \approx 1 \times 10^5$  AADT, and examine a range of  $\alpha_d$  up to  $1.2 \times 10^7$  (\$/lane-mile).

Figure 33 plots the results, including the percentage savings in total life cycle cost as compared to benchmark 2, as well as the percentage of converted lane-miles. If the conversion cost can be reduced to be almost negligible (i.e.,  $\alpha_d = 0$  \$/lane-mile) as advanced technology permits, about 54% of the lane miles will be converted, leading to as much as 25% improvement in systemwide cost savings despite the lighter traffic demand. As expected, the percentage of converted lane-miles decrease as conversion becomes more expensive. The saving will eventually diminish when  $\alpha_d$  exceeds  $8.2 \times 10^6$  (\$/lane-mile).

In this analysis, we also examine the scenario in which the driver cost is deducted (as indicated by the black dashed line in Figure 28a) whenever trucks are platooned. The results exhibit similar trends, but much larger cost reduction can be achieved by platooning. When the conversion cost is negligible, the optimal conversion of about 40% of lane-miles can reduce the total cost by 42.32%. Even when conversion is very costly at  $\alpha_d = 1.2 \times 10^7$  \$/lane-mile, it is still optimal to convert 23.28% of the network lane-miles to achieve a cost reduction of 14.88%.

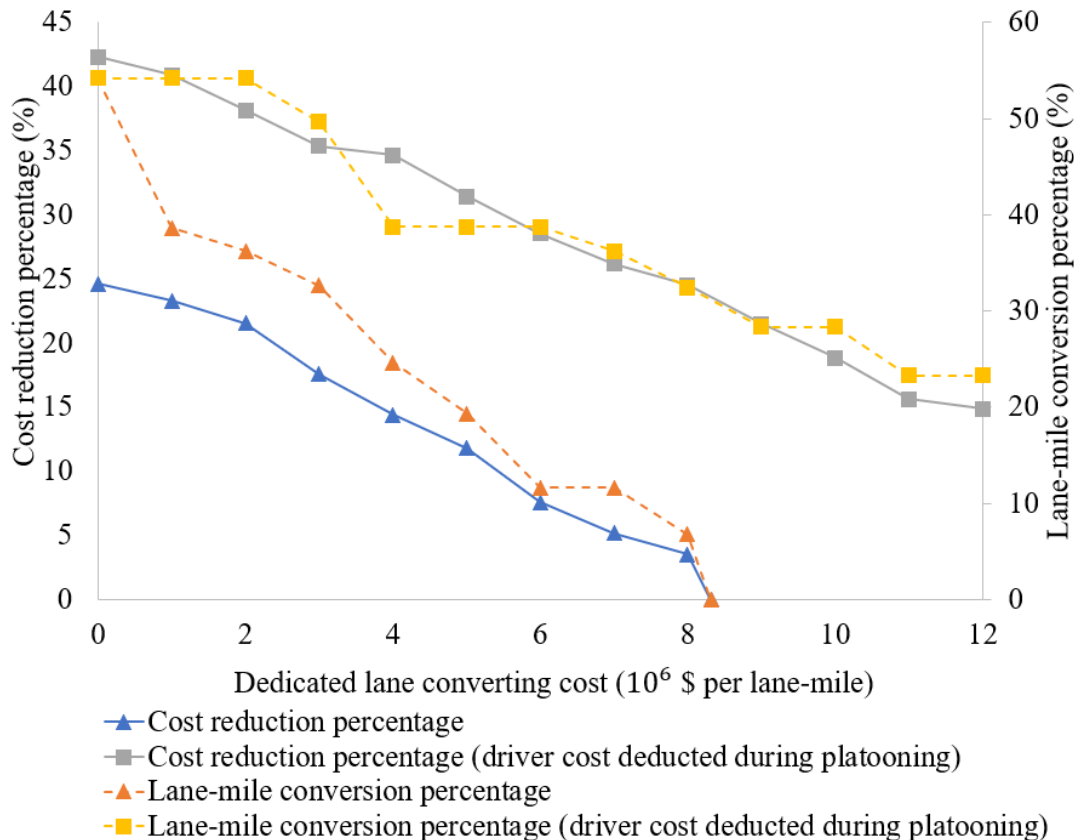


**Figure 33. Graph. Percentages of cost reduction and lane-mile conversion under light demand.**

Next, we set  $\alpha_d = 4 \times 10^6$  (\$/lane-mile) and let the total demand  $\sum_{od} q^{od}$  vary from  $2.5 \times 10^4$  to  $2.5 \times 10^5$  AADT. The resultant percentages of cost saving (again, as compared to their own no-platoon-lane counterparts) and converted lane-mile are plotted in Figure 34. When driver cost is included during platooning, as the demand increases within the chosen range, the cost saving increases at an accelerating rate from around 6.5% to 49.6%. This trend attributes to the congestion penalty on the regular lanes quickly dominating for heavy traffic demand while the cost increment on the platoon lanes is very marginal (and hence traffic flow remains efficient) due to their larger capacity. This result is still conservative because we ignore the presence of background traffic in regular lanes, hence the savings from reducing congestion cost could be even higher. Theoretically, more savings can be achieved under heavier traffic demand, as platoon lanes exhibit strong economies of scale. In contrast, the percentage of converted lane miles appears to increase concavely as the demand increases; this observation indicates diminishing marginal returns from lane conversion after the network design converges to an optimal skeleton. When driver cost is deducted for platooned traffic, the trends are similar; yet the optimal solution tends to convert even more lane-miles to achieve even higher cost savings. Under a very low demand level, 28.3% of lane-miles are converted, resulting in a cost reduction of 22.6%. The cost saving grows to 78.4% as demand increases to  $2.5 \times 10^5$  AADT. All these results illustrate the potential of achieving significant socioeconomic gains from setting up dedicated truck-platoon lanes, especially in regions that expect high truck-traffic demand growth in the long run.

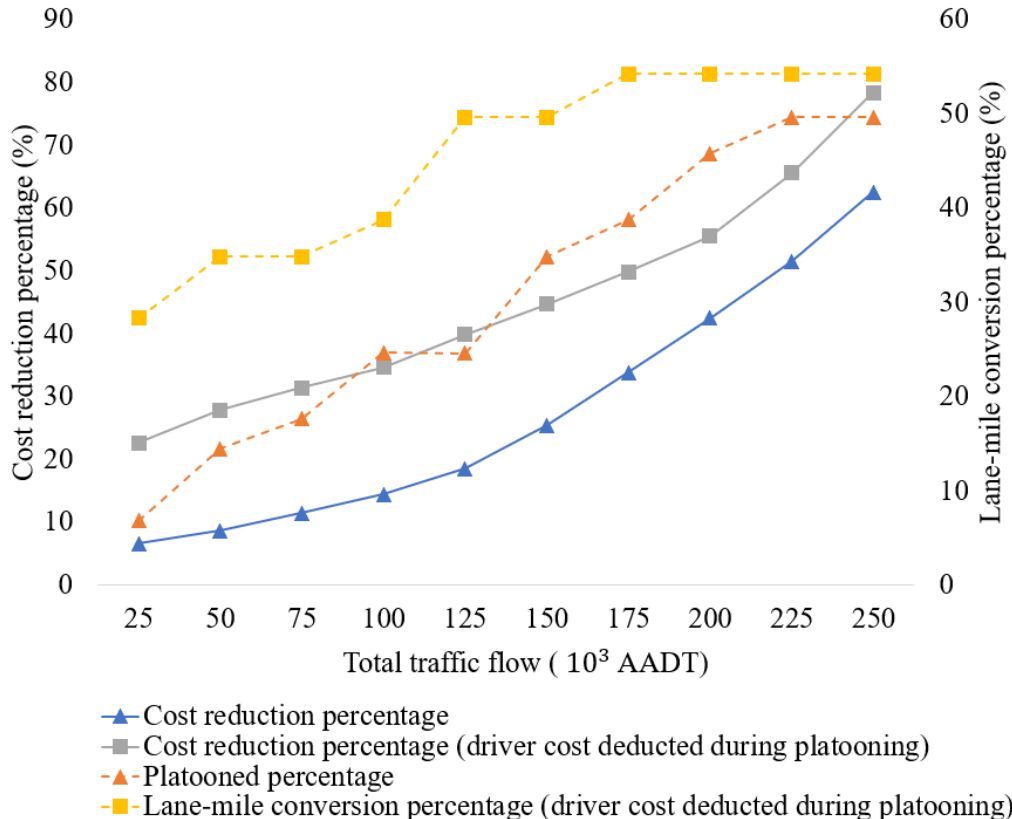


**Figure 34. Graph. Percentages of cost reduction and lane-mile conversion under a range of demand levels.**

## REFERENCES

- [1] Jan Wedemeier Malte Jahn, Paul Schumacher, and André Wolf. Combined transport in Europe: Scenario-based projections of emission saving potentials. *HWI Research Paper, No.192*, 2020.
- [2] Bureau of Transportation Statistics. *Transborder freight data*. Online database, 2020, [www.bts.gov/transborder](http://www.bts.gov/transborder).
- [3] Sadayuki Tsugawa, Shin Kato, and Keiji Aoki. An automated truck platoon for energy saving. In *2011 IEEE/RSJ International Conference on Intelligent Robots and Systems*, pp. 4109–4114. IEEE, 2011.
- [4] Alejandro Alonso Estébanez, Juan José del Coz Díaz, Felipe Pedro Álvarez Rabanal, Pablo Pascual Muñoz, Paulino José García Nieto, et al. Numerical investigation of truck aerodynamics on several classes of infrastructures. *Wind and Structures*, 26 (1), 2018.
- [5] Michael Zabat, Nick Stabile, Stefano Farascaroli, and Frederick Browand. *The aerodynamic performance of platoons: A final report*. Technical report. California PATH, 1995. Retrieved from <https://escholarship.org/uc/item/8ph187fw>.
- [6] Carl Bergenhem, Steven Shladover, Erik Coelingh, Christoffer Englund, and Sadayuki Tsugawa. Overview of platooning systems. In *Proceedings of the 19th ITS World Congress, Oct 22–26, Vienna, Austria*, 2012.
- [7] Anirudh Kishore Bhoopalam, Niels Agatz, and Rob Zuidwijk. Planning of truck platoons: A literature review and directions for future research. *Transportation Research Part B: Methodological*, 107:212–228, 2018.
- [8] Yung-Cheng Lai, Yanfeng Ouyang, and Christopher PL Barkan. A rolling horizon model to optimize aerodynamic efficiency of intermodal freight trains with uncertainty. *Transportation Science*, 42(4):466–477, 2008.
- [9] Osman Erman Gungor, Ruifeng She, Imad L. Al-Qadi, and Yanfeng Ouyang. One for all: Decentralized optimization of lateral position of autonomous trucks in a platoon to improve roadway infrastructure sustainability. *Transportation Research Part C: Emerging Technologies*, 120:102783, 2020.
- [10] Hossein Noorvand, Guru Karnati, and B. Shane Underwood. Autonomous vehicles: Assessment of the implications of truck positioning on flexible pavement performance and design. *Transportation Research Record*, 2640(1):21–28, 2017.
- [11] Daquan Sun, Guoqiang Sun, Xingyi Zhu, Alvaro Guarin, Bin Li, Ziwei Dai, and Jianming Ling. A comprehensive review on self-healing of asphalt materials: Mechanism, model, characterization and enhancement. *Advances in Colloid and Interface Science*, 256:65–93, 2018.
- [12] Osman Erman Gungor and Imad L. Al-Qadi. Wander 2D: A flexible pavement design framework for autonomous and connected trucks. *International Journal of Pavement Engineering*, pp. 1–16, 2020.
- [13] Sadayuki Tsugawa, Sabina Jeschke, and Steven E. Shladover. A review of truck platooning projects for energy savings. *IEEE Transactions on Intelligent Vehicles*, 1(1):68–77, 2016.

- [14] Leila Hajibabai, Yun Bai, and Yanfeng Ouyang. Joint optimization of freight facility location and pavement infrastructure rehabilitation under network traffic equilibrium. *Transportation Research Part B: Methodological*, 63:38–52, 2014.
- [15] Erik Larsson, Gustav Sennton, and Jeffrey Larson. The vehicle platooning problem: Computational complexity and heuristics. *Transportation Research Part C: Emerging Technologies*, 60:258–277, 2015.
- [16] Fengqiao Luo, Jeffrey Larson, and Todd Munson. Coordinated platooning with multiple speeds. *Transportation Research Part C: Emerging Technologies*, 90:213–225, 2018.
- [17] Vadim Sokolov, Jeffrey Larson, Todd Munson, Josh Auld, and Dominik Karbowski. Maximization of platoon formation through centralized routing and departure time coordination. *Transportation Research Record*, 2667(1):10–16, 2017.
- [18] Mohamadhossein Noruzoliaee, Bo Zou, and Yan Joann Zhou. Truck platooning in the US national road network: A system-level modeling approach. *Transportation Research Part E: Logistics and Transportation Review*, 145:102200, 2021.
- [19] Sun, Xiaotong and Yin, Yafeng, An Auction Mechanism for Platoon Leader Determination in Single-Brand Cooperative Vehicle Platooning (2020). Available at SSRN: <https://ssrn.com/abstract=3805126> or <http://dx.doi.org/10.2139/ssrn.3805126>.
- [20] Sun, Xiaotong and Yin, Yafeng, Decentralized Game-Theoretical Approaches for Behaviorally-Stable and Efficient Vehicle Platooning (2021). Available at SSRN: <https://ssrn.com/abstract=3806796> or <http://dx.doi.org/10.2139/ssrn.3806796>.
- [21] Humphreys, Hugh, and David Bevly. Computational fluid dynamic analysis of a generic 2 truck platoon. No. 2016-01-8008. SAE Technical Paper, 2016.
- [22] John Matsson. *An Introduction to ANSYS Fluent 2020*. SDC Publications, 2020. ISBN: 1630574627.
- [23] Matthew Barth, Theodore Younglove, and George Scora. *Development of a heavy-duty diesel modal emissions and fuel consumption model*. Technical report. California PATH, 2005.
- [24] Weihua Gu, Yanfeng Ouyang, and Samer Madanat. Joint optimization of pavement maintenance and resurfacing planning. *Transportation Research Part B: Methodological*, 46(4):511–519, 2012.
- [25] Yanfeng Ouyang and Samer Madanat. Optimal scheduling of rehabilitation activities for multiple pavement facilities: exact and approximate solutions. *Transportation Research Part A: Policy and Practice*, 38(5):347–365, 2004.
- [26] William G. Holland. *Life-cycle cost analysis for road construction contracts*. Technical report. Illinois Department of Transportation, 2012.
- [27] Laura E. Ghosh, Liqun Lu, Hasan Ozer, Yanfeng Ouyang, and Imad L. Al-Qadi. Effects of pavement surface roughness and congestion on expected freeway traffic energy consumption. *Transportation Research Record*, 2503(1):10–19, 2015.
- [28] Osman Erman Gungor and Imad L. Al-Qadi. All for one: Centralized optimization of truck platoons to improve roadway infrastructure sustainability. *Transportation Research Part C: Emerging Technologies*, 114:84–98, 2020.

- [29] Robert Chamberlin, Ben Swanson, Eric Talbot, Jeff Dumont, and Stephen Pesci. Analysis of MOVES and CMEM for evaluating the emissions impact of an intersection control change. In *Transportation Research Board 90<sup>th</sup> Annual Meeting*, 2011.
- [30] Liu, Jun, K. Kockelman, and Aqshems Nichols. "Anticipating the emissions impacts of smoother driving by connected and autonomous vehicles, using the MOVES model." In *Transportation Research Board 96<sup>th</sup> annual meeting*. 2017.
- [31] Yanfeng Ouyang and Samer Madanat. An analytical solution for the finite-horizon pavement resurfacing planning problem. *Transportation Research Part B: Methodological*, 40(9):767–778, 2006.
- [32] Osman Erman Gungor, Antoine Michel Alain Petit, Junjie Qiu, Jingnan Zhao, Hadi Meidani, Hao Wang, Yanfeng Ouyang, Imad L Al-Qadi, and Justan Mann. Development of an overweight vehicle permit fee structure for illinois. *Transport Policy*, 82:26–35, 2019.
- [33] AASHTO. *Mechanistic-Empirical Pavement Design Guide: A Manual of Practice*. AASHTO, 2008.
- [34] Heinz Spiess. Conical volume-delay functions. *Transportation Science*, 24(2):153–158, 1990.
- [35] Adamou Ouorou, Philippe Mahey, and J-Ph Vial. A survey of algorithms for convex multicommodity flow problems. *Management Science*, 46(1):126–147, 2000.
- [36] Giorgio Gallo, Claudio Sandi, and Claudio Sodini. An algorithm for the min concave cost flow problem. *European Journal of Operational Research*, 4(4):248–255, 1980.
- [37] Michael Patriksson. *The traffic assignment problem: models and methods*. Courier Dover Publications, 2015.
- [38] Andreas Wächter and Lorenz T. Biegler. On the implementation of an interior-point filter line-search algorithm for large-scale nonlinear programming. *Mathematical Programming*, 106(1):25–57, 2006.
- [39] Peter J.M. Van Laarhoven and Emile H.L. Aarts. *Simulated Annealing: Theory and Applications*. Springer, 1987.
- [40] Federal Highway Administration. *Status of the Nation's Highways, Bridges, and Transit*. Courier Dover Publications, 2015.
- [41] Mojtaba Ziyadi, Hasan Ozer, Seunggu Kang, and Imad L. Al-Qadi. Vehicle energy consumption and an environmental impact calculation model for the transportation infrastructure systems. *Journal of Cleaner Production*, 174:424–436, 2018.
- [42] Transportation Research Board. *Highway capacity manual 2000*. National Research Council, 2000.
- [43] Dan Murray and Seth Glidewell. *An analysis of the operational costs of trucking: 2019 update*. Technical report. International Transport Research Documentation, 2019.
- [44] Michael Evans, Ryan Marchildon, and Simon A.M. Hesp. Effects of physical hardening on stress relaxation in asphalt cements: Implications for pavement performance. *Transportation Research Record*, 2207(1):34–42, 2011.

- [45] Francisco Dalla Rosa, Litao Liu, and Nasir G. Gharaibeh. IRI prediction model for use in network-level pavement management systems. *Journal of Transportation Engineering, Part B: Pavements*, 143(1):04017001, 2017.
- [46] Imad L. Al-Qadi, Egemen Okte, Aravind Ramakrishnan, Qingwen Zhou, and Watheq Sayeh. *Truck-platoonable pavement sections in Illinois' network*. Technical report. Illinois Center for Transportation, FHWA-ICT-21-002, 2021.